Application note

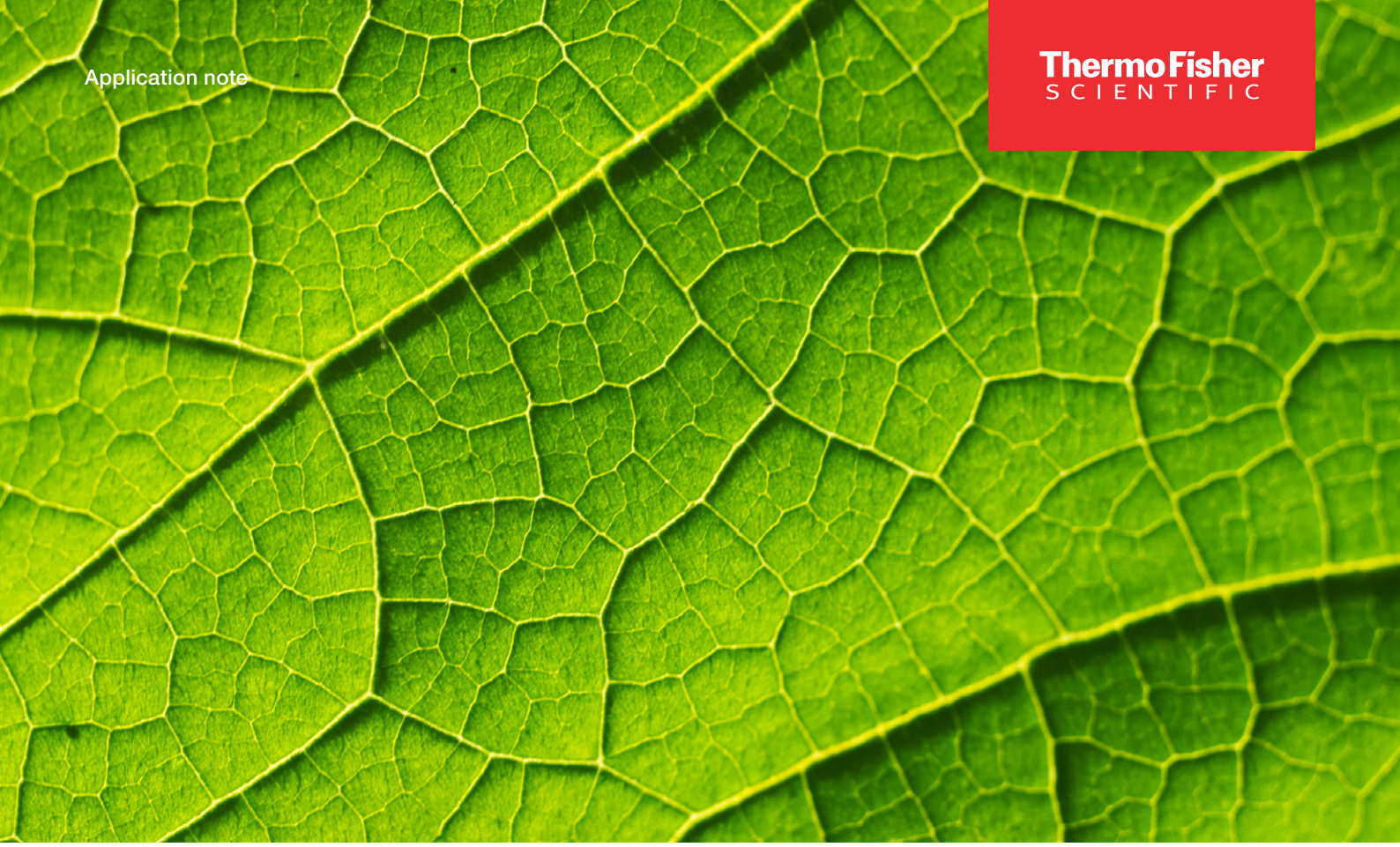

Analyzing Leaf Pigmentation Through Combined Raman / Photoluminescence Spectroscopy

Author

Matthew Gabel, Ph.D.

Industry/Application

Botanical, Raman spectroscopy, photoluminescence imaging

Product used

Thermo Scientific™ DXR3xi Raman imaging Microscope

Goal

Demonstrate the advantages of combined Raman / photoluminescence spectroscopy and imaging

Key Analytes

Botanical pigmentation

Key Benefits

Combining the high speed of photoluminescence mapping with the great specificity of Raman spectroscopy provides a sophisticated non-invasive method to analyze the states of plants' conditions.

Introduction

As a laser excitation-driven technique, Raman spectroscopy naturally goes hand-in-hand with other analytical techniques based on the interaction of light and matter, such as photoluminescence (PL) spectroscopy. PL is a technique measuring the electromagnetic emittance of chemical structures after absorbing incident light; it is commonly used for cell imaging, studying semiconductor structures such as quantum wells, and monitoring diamond purity and defects, among other applications.[1,2] Given the much higher efficiency of PL processes (compared to Raman), it is a faster imaging technique that can be combined with Raman spectroscopy on a single instrument to provide more detailed material understanding of many PL-active materials, including biological samples such as leaves.

The botanical structure for nutrient transport in the leaves' veins and midribs[3] has a distinct Raman signature and PL signal from the main surface of the leaves' blades. This is due to different pigmentation across the leaves' surface. Raman spectra can be used to measure (*in vivo*) the health of a plant,[4] and combining this with PL mapping can enhance these assessment capabilities. In this work, the correlation of Raman spectra to the PL data validates the use of PL mapping as a substitute to the slower Raman mapping; individual point Raman spectra coupled with large-area PL maps provide high sample specificity and information with rapid large-scale analysis.

The Thermo Fisher DXR3xi Raman Imaging Microscope was used to capture this data. A 532 nm excitation laser equipped with extended range grating (50-6000 cm^{-1} / 532-781 nm) was used for the PL measurements while a 785 nm excitation laser was used for the Raman measurements. Since the leaves have a strong fluorescence signal which can overwhelm the Raman intensity, it requires the Raman data to be collected with this lower-fluorescence 785 nm wavelength. Various leaves are studied here (Figure 1), with both large-area PL maps, as well as spatially correlated Raman and PL spectra. This work maps large areas using the more rapid PL imaging while correlating these images with Raman spectral data averaged over a number of points on the regions of interest. Once a sample is placed in the instrument and a visual image has been captured, both the PL and Raman data can be taken without having to move the sample; the excitation laser simply needs to be exchanged between the measurements. The typical PL signal in plants (from chlorophyll) consists of two peaks at 685-690 and 730-740 nm.[5] Meanwhile, there are many Raman peaks in the plant spectra: Some major peaks can be identified from the carotenoid structures at 1525 cm^{-1}, 1157cm^{-1}, and 1005 cm^{-1} along with chlorophyll peaks at 1604 cm^{-1} and 1327 cm^{-1} and cellulose peaks at 2892 cm^{-1} and 1096 cm^{-1}.[6]

Figure 1. Clockwise from top left: Pleroma, Ivy, and Japanese Laurel leaves.

Pleroma Leaf – Structural Elements

The first leaf studied under the above experimental conditions, a pleroma leaf, shows distinct PL spectra of the different structural elements in the leaf (the ribs, veins, and blade), revealing fine vein structures (on the order of 100 microns in width) that cannot be distinguished from the blade optically (Figure 2A, 2B). This is a rapid large-area scan with high spatial resolution PL spectral information (pixel size of 25 microns) showing very distinct chlorophyll peaks (Figure 2C).

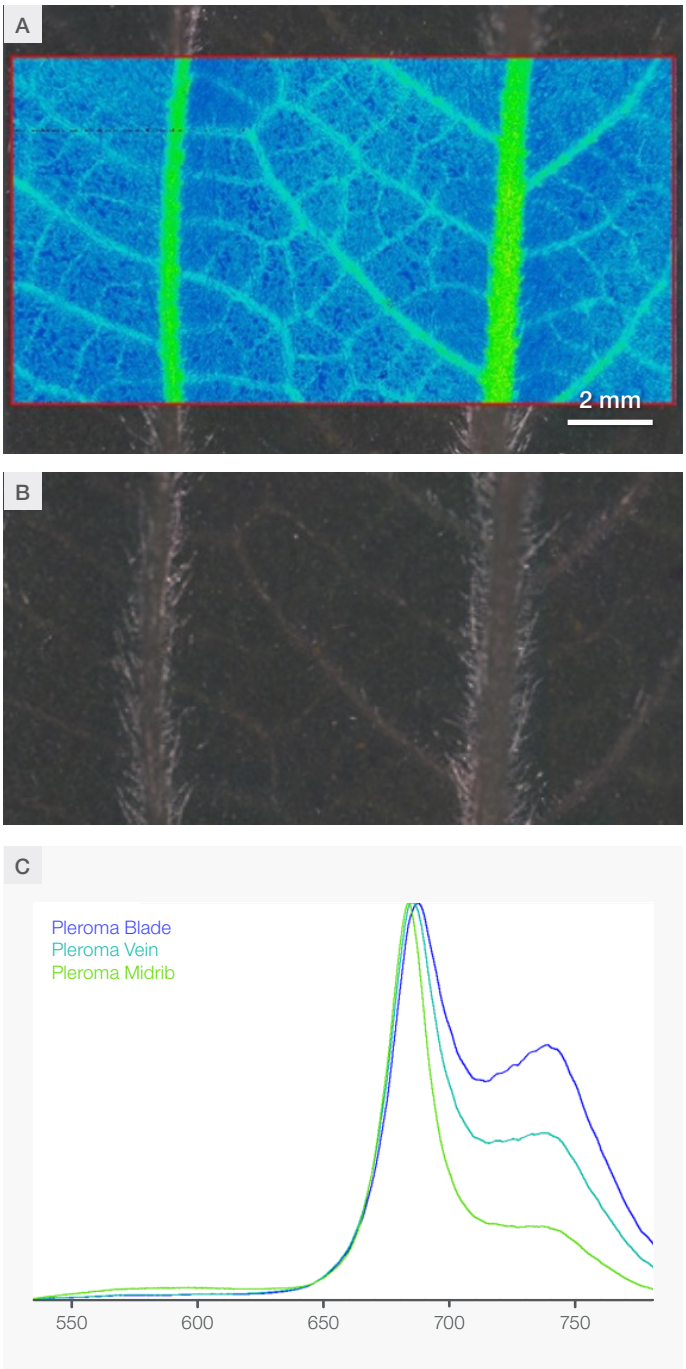

Figure 2. (A) A false-color PL map (16 x 8.5 mm, 220k spectra, 30 minutes) of the midrib, veins, and blade of a pleroma leaf. The color scale corresponds to a peak ratio between the 690 and 740 nm peaks where green is a largest ratio and blue is the smallest. (B) The optical image underlying the PL map. (C) The distinct PL spectra (color correlated) with three map regions.

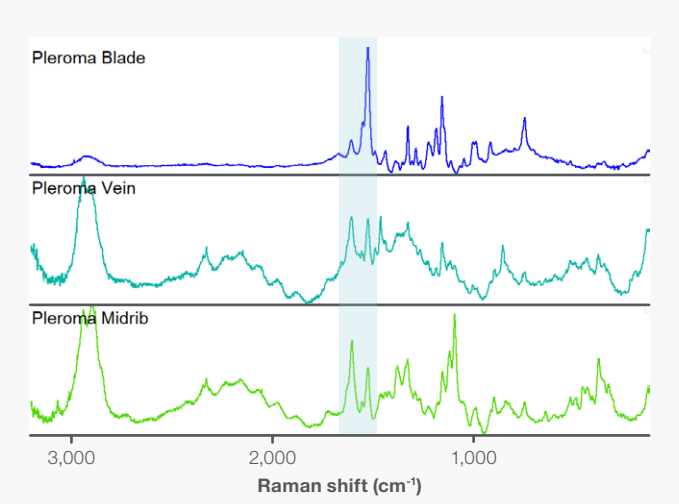

Figure 3. Baseline corrected Raman spectra collected from a pleroma leaf, including the blade, vein, and midrib matching the regions in Figure 2C. The highlighted region emphasizes a changing ratio between the dominant chlorophyll peak at 1604 cm^{-1} and the main carotenoid peak at 1525 cm^{-1}.

While PL mapping is an excellent technique for large area scanning (collecting approximately 500x faster than Raman spectral mapping with the same area and spatial resolution), it does not convey as much structural / molecular information as Raman spectroscopy (Figure 3). The Raman spectra of the various structural elements show a strong carotenoid presence in the blade of the leaf, with a fairly equal ratio of carotenoid and chlorophyll in the veins and a stronger ratio of chlorophyll in the rib. Additionally, there is a much stronger cellulose signal in the veins and rib than there is in the blade, correlating with the stronger structural support in those elements. Being able to switch between Raman and PL collection modes on a single instrument with no need to change the sample constitutes a major analytical advantage. Combining information from both techniques, the different leaf structures can be catalogued by the distinct pigmentation ratios of the main carotenoid (1525 cm^{-1}) and chlorophyll (1604 cm^{-1}) peaks, alongside the PL peak ratios - see Table 1.

Feature	Blade	Vein	Rib
PL (690 nm : 740 nm ratio)	1.471	1.938	5.207
Raman (1604 cm^{-1} : 1525 cm^{-1} ratio)	0.184	1.094	1.543

Table 1. Peak ratios between the two main chlorophyll peaks from the PL spectra as well as the peak ratio between the main Raman peaks for chlorophyll at 1604 cm^{-1} and carotenoid at 1525 cm^{-1}.

However, there are occasionally components in the study of botanicals for which the PL signal of chlorophyll may not be useful—for example, a single droplet of sap along the rib of the leaf (Figure 4).

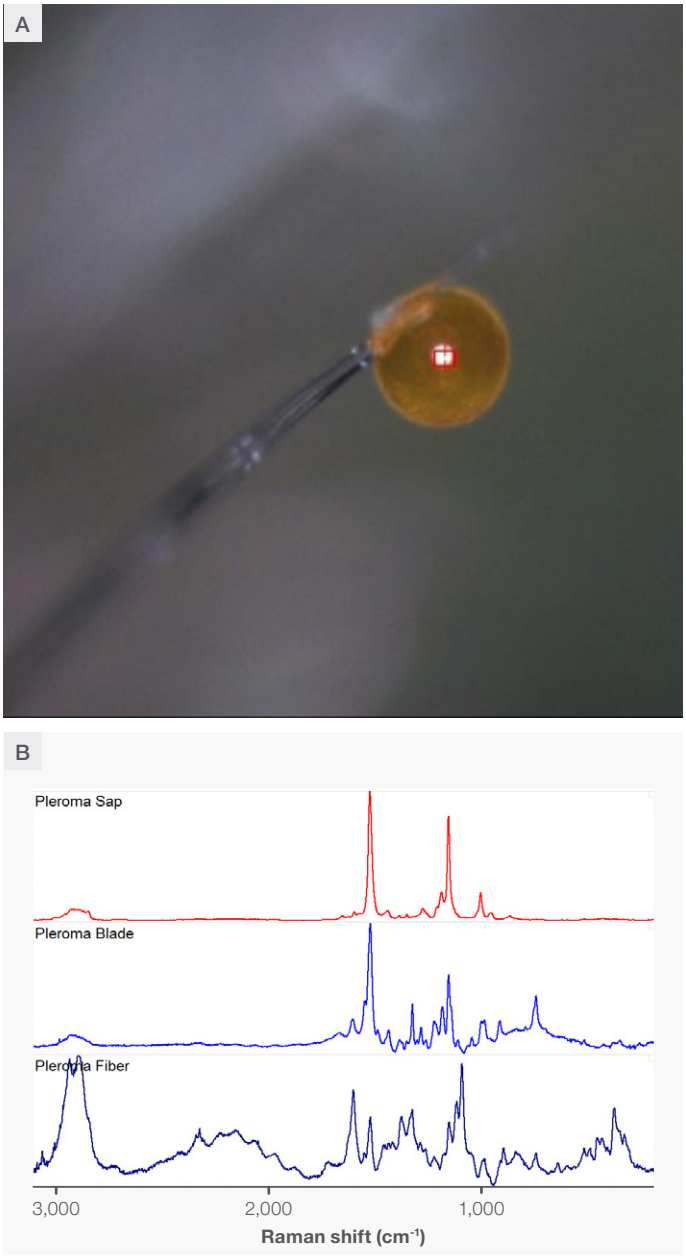

Figure 4. (A) The droplet has a diameter of 15 um while the fiber it is suspended on has a width of 3 um. (B) Baseline corrected Raman signals for the fiber and droplet seen in Figure 4A. In comparison, the blade spectrum from Figure 3 has a significant contribution from the droplet, although there are other components as well.

The droplet appears to be almost completely comprised of carotenoid pigment, strongly representing all three carotenoid Raman peaks at 1525, 1157 and 1005 cm^{-1}. The lack of any chlorophyll in this sap precludes the chlorophyll-based PL spectroscopy as an analytical method for this specific element. Fortunately, by utilizing both Raman and PL it is easy to swap to a more appropriate technique for the necessary analysis. Spectral similarities between the droplet and blade confirm the previous assertion that the blade contains more carotenoid than the midrib or veins (which predominately carry chlorophyll). The combination of chlorophyll PL mapping and detailed Raman study of carotenoid and chlorophyll distribution builds up a basic understanding of the correlation between PL and Raman signals in botanical structures.

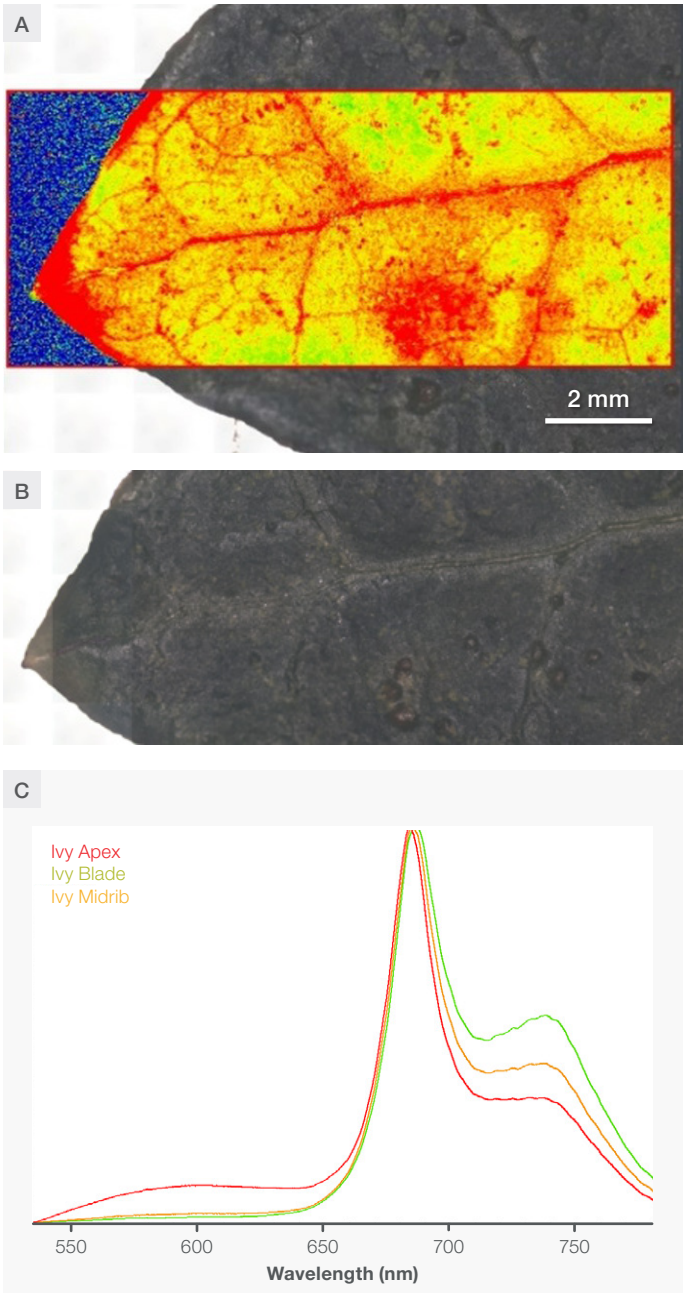

Figure 5. (A) A false-color PL map of an ivy leaf showing the midrib out to the apex of the leaf. The color scale corresponds to a peak ratio between the 690 and 740 nm peaks where red is a largest ratio and green in the smallest. (B) The optical image underlying the PL map. (C) The distinct PL spectra (color correlated) with three map regions. The discolored apex region has a third, weak PL peak centered at 600 nm.

Ivy Leaf – Surface Damage

This PL / Raman relationship can be used to analyze other features in botanical samples as well, not just the basic leaf structure. A second image here is from an ivy leaf with the same PL (Figure 5) and Raman (Figure 6) tests as the previous pleroma leaf. In Figure 5 the ivy leaf displayed regions of damage and discoloration such as a dried / light brown surface at the apex of the leaf (Figure 5B) which corresponds to the development of a third PL peak (Figure 5C). The Raman signal from the apex region (Figure 6) shows the presence of the chlorophyll peaks after damage, but very little carotenoid signal. The blade has a chlorophyll to carotenoid peak ratio of 0.67 while the midrib has a ratio of 1.17 and the apex has a ratio of 10.42 (see Table 2).

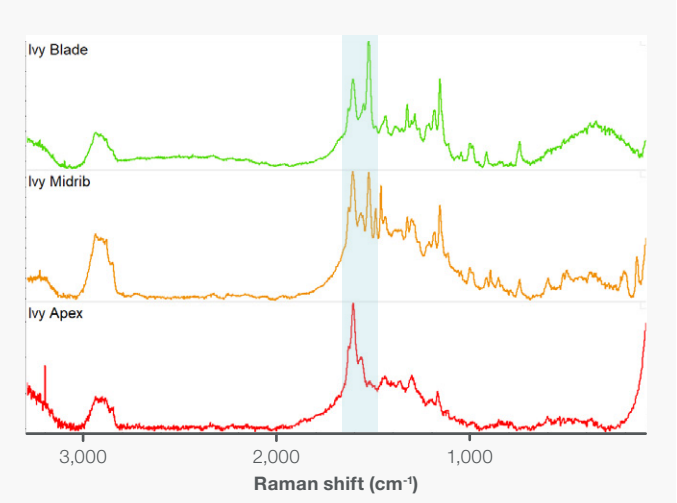

Figure 6. Baseline corrected Raman spectra correlating to the collected PL regions in Figure 5C. The highlighted region emphasizes a ratio between the dominant chlorophyll peak at 1604 cm^{-1} and the main carotenoid peak at 1525 cm^{-1}, revealing almost no carotenoid signal remining in the damaged region at the apex.

Feature	Blade	Rib	Apex
PL (690 nm : 740 nm ratio)	1.849	2.445	3.377
Raman (1604 cm^{-1} : 1525 cm^{-1} ratio)	0.667	1.168	10.423

Table 2. Peak ratios between the two main chlorophyll peaks from the PL spectra as well as the peak ratio between the main Raman peaks for chlorophyll at 1604 cm^{-1} and carotenoid at 1525 cm^{-1}.

In botanical samples, surface irregularities are especially interesting points of study, and both the Raman and PL data show interesting spectral feature in the damaged region as compared to the standard structural elements.

Japanese Laurel Leaf – Multihued Samples

Finally, unlike the previous two samples, the Japanese laurel has a naturally multihued leaf with regions of green and white pigmentation across the blade. A PL map (Figure 7) reveals a clear difference between the pigment regions and, similar to the apex of the ivy leaf, a third signature PL peak around 590 nm unique to the white pigmentation region.

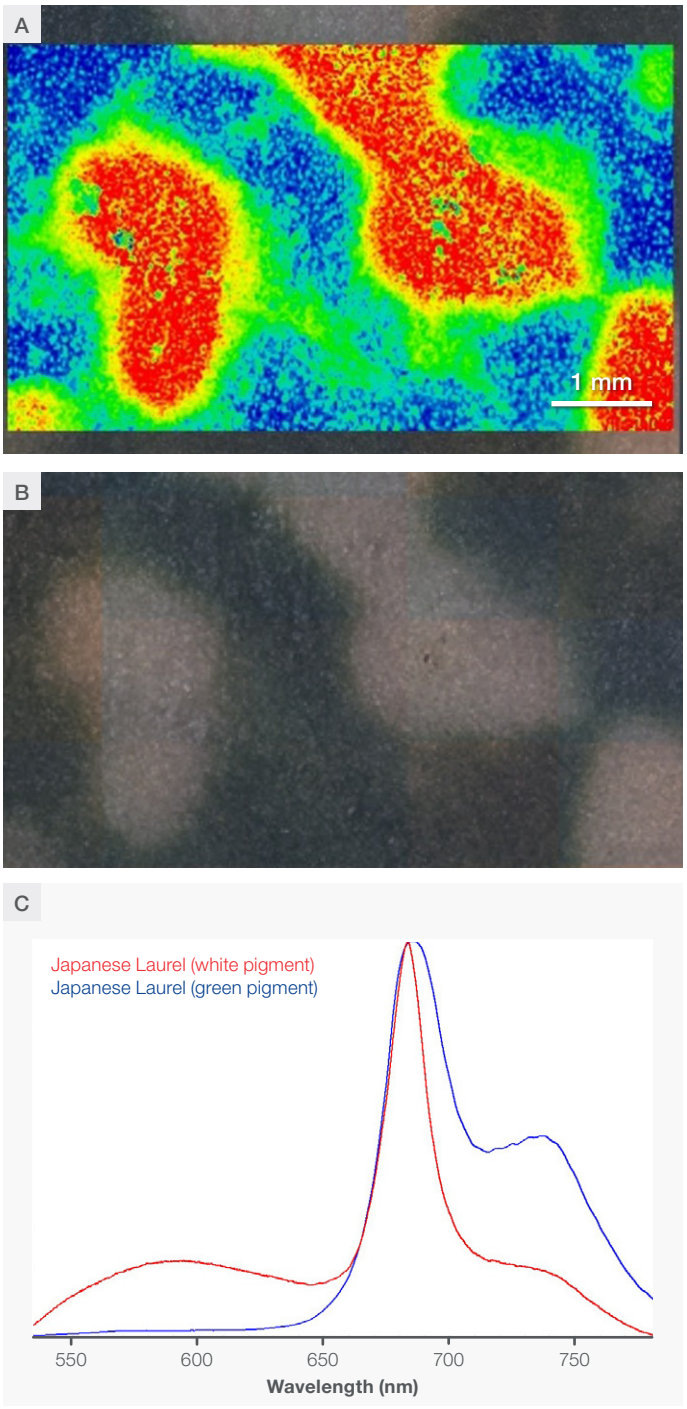

Figure 7. (A) A false-color PL map of a Japanese laurel leaf showing the distinct pigmented spotting on the leaf surface. The color scale corresponds to a peak ratio between the 690 and 740 nm peaks where red is the largest ratio and blue is the smallest. (B) The optical image underlying the PL map. (C) The distinct PL spectra (color correlated) with the two map regions shows the difference between the pigments – note that the white pigment has a tertiary PL peak at 590 nm.

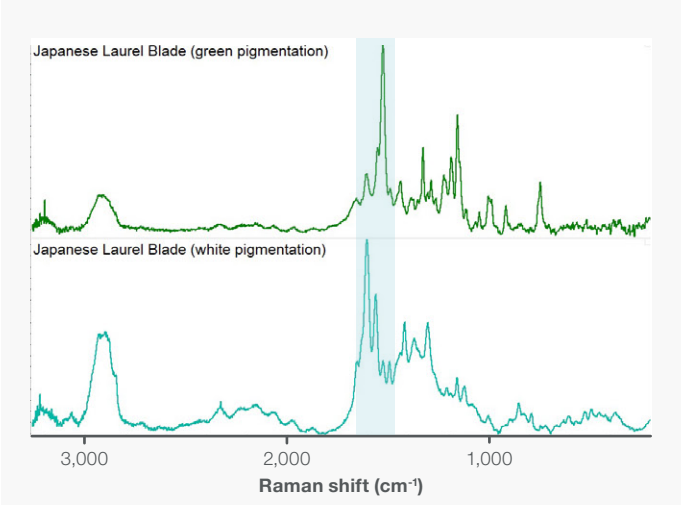

Figure 8. Baseline corrected Raman spectra correlating to the collected PL regions in Figure 7B. The "fingerprint" region between 800 and 1600 cm^{-1} reveals very distinct structures associated with the pigments, as well as a strong shift in the chlorophyll to carotenoid ratio (in the highlighted region).

Feature	White Region	Green Region
PL (690 nm : 740 nm ratio)	5.349	1.873
Raman (1604 cm^{-1} : 1525 cm^{-1} ratio)	5.357	0.233

Table 3. Peak ratios between the two main chlorophyll peaks from the PL spectra as well as the peak ratio between the main Raman peaks for chlorophyll at 1604 cm^{-1} and carotenoid at 1525 cm^{-1}.

The different pigmentation regions have a huge Raman response (Figure 8) with much more chlorophyll in the white region. This is indicated by a chlorophyll to carotenoid ratio of 5.36, compared to the ratio value of 0.23 for the green pigmentation (see Table 3).

Conclusions

Photoluminescent and Raman measurements both provide valuable information in their own right, but give a much deeper understanding of the botanical pigmentation when combined in a single analytical instrument. The high speed of the chlorophyll PL mapping makes it an excellent initial resource, although the greater specificity in the Raman peaks is necessary in order to conduct deeper studies, such as a direct comparison of the intensities of carotenoid and chlorophyll pigmentation. The distribution of pigmentation can be tracked through various leaf structures and surface features in these high spectral and spatial resolution maps. These measurements can eventually be used to provide valuable information about the state of the plant's condition and health with quick, non-invasive analytical methods.

Citations

1. Teets, T. S. (2021). Photoluminescence. In ACS in focus. *https://doi.org/10.1021/acsinfocus.7e5014*
2. Thermo Fisher Scientific. (2024). Distribution of Defects & Impurities in Diamonds Probed by Infrared and Photoluminescence Imaging. Application Note. *https://assets.thermofisher.com/TFS-Assets/CAD/Application-Notes/vib-defects-in-diamonds-app-Note.pdf*
3. Da Silva, N. R., Florindo, J. B., Gómez, M. C., Rossatto, D. R., Kolb, R. M., & Bruno, O. M. (2015). Plant identification based on leaf midrib Cross-Section images using fractal descriptors. PloS One, 10(6), e0130014. *https://doi.org/10.1371/journal.pone.0130014*
4. Altangerel, N., Ariunbold, G. O., Gorman, C., Alkahtani, M., Borrego, E. J., Bohlmeyer, D., Hemmer, P., Kolomiets, M. V., Yuan, J. S., & Scully, M. O. (2017). In vivo diagnostics of early abiotic plant stress response via Raman spectroscopy. Proceedings of the National Academy of Sciences of the United States of America, 114(13), 3393–3396. *https://doi.org/10.1073/pnas.1701328114*
5. Huemmrich, K. F., Campbell, P. K. E., Zesati, S. a. V., Sackett, S. E., Unger, S., May, J. L., Tweedie, C. E., & Middleton, E. M. (2022). Leaf-level chlorophyll fluorescence and reflectance spectra of high latitude plants. Environmental Research Communications, 4(3), 035001. *https://doi.org/10.1088/2515-7620/ac5365*
6. Rys, M., Szaleniec, M., Skoczowski, A., Stawoska, I., & Janeczko, A. (2015). FT-Raman spectroscopy as a tool in evaluation the response of plants to drought stress. Open Chemistry, 13(1). *https://doi.org/10.1515/chem-2015-0121*

Learn more at **thermofisher.com/raman**